Chem Soc Rev

Chemical energy dissipation at surfaces under UHV and higher pressure conditions studied using metal- insulator-metal and similar devices

Journal:	*Chemical Society Reviews*
Manuscript ID	CS-REV-12-2015-000932.R1
Article Type:	Review Article
Date Submitted by the Author:	29-Mar-2016
Complete List of Authors:	Diesing, Detlef; Universität Duisburg-Essen, Fakultät Für Chemie Hasselbrink, Eckart; Universitat GH Essen - FB8, Inst. f. Physikal.u.Theoret. Chemie

Journal Name

ARTICLE TYPE

Cite this: DOI: 10.1039/xxxxxxxxxx

Chemical energy dissipation at surfaces under UHV and higher pressure conditions studied using metal-insulator-metal and similar devices†

Detlef Diesing[b] and Eckart Hasselbrink[a]

Received Date
Accepted Date

DOI: 10.1039/xxxxxxxxxx

www.rsc.org/journalname

Metal heterostructures have in recent years been used to gain insights into the relevance of energy dissipation into electronic degrees of freedom in surface chemistry. Non-adiabaticity in the surface chemistry results in the creation of electron-hole pairs, the number and energetic distribution of which needs to be studied in detail. Several types of devices such as metal-insulator-metal, metal-semiconductor and metal-semiconductor oxide-semiconductor, have been used. These devices operate by spatially separating the electrons form the holes, as an internal barrier allows only – or at least favours – for one kind of carriers the transport from the top to the back electrode. An introduction into the matter, a survey of the literature and a critical discussion of the state of research is attempted.

1 Introduction

Metal-insulator-metal, metal-insulator-semiconductor and metal-semiconductor thin film devices have in recent years allowed to shed new light on a long standing, fundamental problem in surface chemistry. For more or less pragmatic reasons it has been commonly assumed that the dynamics of reactions at metal surfaces proceeds strictly in the electronic ground state. It is argued that excited electronic states have short lifetimes, hence exhibit broad widths leading to a large coupling between states such that the system will rapidly collapse onto the electronic ground state. However, this argument may also be turned around. As metals have a continuous spectrum of electronic excitations, no chemical process on a metallic surface will proceed without any excitation of electron-hole pairs.[1] Hence, it remains the quest to quantify the extent of energy which is transferred into electronic excitations in the course of a surface chemical reaction. Thin film heterostructures have just made such studies possible.

Moreover, there is also a strong applied interest in this question. Any excitation of electronic degrees of freedom in the metal substrate can be regarded as a direct conversion of chemical energy into electrical energy. And the question arises if these processes are such strong that they promise to be practical applicable for the generation of electricity.[2,3] Such an utilisation will require to operate chemical reactors at large turn over frequencies, implying rather high pressures of the reacting gases and elevated temperatures. Hence, this is the motivation for experiments at conditions closely resembling these.

The fundamental aspect of the functionality of thin metal heterostructures in this context is, that the structure allows to spatially separate the excited electrons from the corresponding holes (Fig. 1). Hence, a current can be observed when connecting a meter between the front metal layer and the back side which is a reflection of the number of electronic excitations created by the surface chemistry per unit time.

The role of non-adiabaticity in surface chemical reactions has recently been reviewed.[4–6] A review with special focus on the interplay of hot electrons and metal-oxide interfaces in the context of catalysis has also been prepared recently.[7]

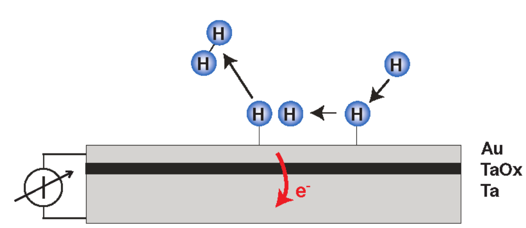

Fig. 1 Principle of the application of thin metal film devices for the study of the coupling to electronic degrees of freedom in surface chemistry. The chemistry proceeding on the front side goes along with the excitation of electron-hole-pairs, the electrons of which may in this case pass the barrier imposed by the oxide layer provided they have sufficient energy. The resulting electron flux can externally be detected as a macroscopic current.

[a] Address, Fakultät f. Chemie, Universität Duisburg-Essen, 45141 Essen, Germany. Fax: +49 201 1833228; Tel: +49 201 1833056; E-mail: Eckart.Hasselbrink@Uni-Duisburg-Essen.de
[b] Address, Fakultät f. Chemie, Universität Duisburg-Essen, 45141 Essen, Germany.
† Electronic Supplementary Information (ESI) available: [details of any supplementary information available should be included here]. See DOI: 10.1039/b000000x/

2 Devices

In recent years, several laboratories have made use of structures which have in common that a several nanometer thick metal film is exposed to vacuum and its surface supports the chemistry to study, while an internal interface serves as a filter for either electron or hole transport. The metal film rests either on a substrate with a thin oxide layer at the interface or alternatively the spontaneously formed Schottky space charge layers at metal-semiconductor interfaces have been utilised as such barrier layers. Metal-insulator-metal (MIM) structures have been prepared by us by first electrochemically oxidising a 30 nm thick metal film deposited on glass.[8–10] The oxidation process is self-limiting, resulting in a uniform oxide thickness of 3-4 nm.[11] On top of this oxide layer a metal film is deposited with a thickness just large enough to ensure that the film is closed. Thicknesses of 15 nm for Au and 7 nm for Pt have been sufficient to achieve the latter. These films are microcrystalline in structure.

The band structure of such a device is illustrated in Fig. 2. If no bias voltage is applied to the device the Fermi levels of the top metal film and the substrate align. These two systems are separated by the oxide layer which exhibits a band gap. For the barrier materials used by us, Ta, Al and Ti, the width of the band gap ranges between 3 and 5 eV.[12,13] The band gap is energetically aligned such with the Fermi level of the metal that the conduction band is closer to the Fermi level than the valence band. Thus, the energy with respect to the band edge required for transport is smaller for electrons than for holes. Moreover, we find a built-in electric field across the oxide causing the barrier to be skewed like a parallelogram. I.e the barrier for electrons is larger on the interface towards the top metal film than towards the substrate.

The carrier transport though such systems was characterised studying the optical response to near-infrared photons.[14] The most important finding was that for excitation energies close to the barrier height always electron transport from the top metal to the substrate was favoured over the reverse transport. This effect was tentatively attributed to energy losses due to electron-phonon scattering in the oxide's conduction band.

Metal–semiconductor (MS) structures have also been used to study the conversion of chemical energy into electronic excitations in the course of surface reactions.[2,15,16] In these structures a Schottky barrier at the buried interface serves as filter for (hot) electrons or alternatively holes (Fig. 3). It depends on the doping of the semiconductor substrate whether its bands bend up (n-type semiconductor) or bend down (p-type) at the interface due to the formation of a space charge layer. That creates a barrier for electron transport at energies close to the conduction band minimum or alternatively for holes at the valence band top. In the first case, this Schottky barrier allows only electrons with excitation energies larger than the barrier height to cross into the conduction band of the semiconductor substrate, whereas the corresponding holes are confined at the interface. In the second case, the role of electrons and holes is reversed.

These structures have in common that a buried oxide layer or alternatively the Schottky barrier serves to separate the chemically excited (hot) electrons from the corresponding holes. As long as the thickness of the top metal film is small enough that the transport to the internal interface is predominantly ballistic – a phrase standing for not encountering inelastic collisions – these devices can be utilised to quantify the electronic excitations arising from the chemistry at the vacuum interface. Schottky barriers typically exhibit heights of 0.5-0.8 eV and the space charge layer extends ≈100 nm into the semiconductor substrate. Hence, tunnelling is exceedingly improbable and the barrier acts as a filter with a sharp threshold energy. However, this statement need to be softened as in laboratory devices the Schottky barrier typically exhibits a lateral variation of 0.1 - 0.2 eV. MIM and metal-insulator-semicondutcor (MIS) devices utilise a nanometer-thick oxide layer which serves as charge carrier filter, however, with a threshold energy typically larger than 1 eV. Tunnelling allows carriers with energies somewhat smaller than the barrier to pass the latter. Hence, the filter cuts off less sharply. Moreover, MIM devices allow electrons and holes of sufficient energy to pass the barrier. However, the threshold energies differs for electrons and holes, such that transport for one of the two will predominate.

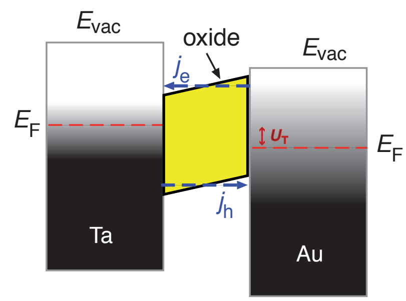

Fig. 2 Bandstructure of a Au-Ta metal-insulator-metal thin film device. The oxide layer exhibits a bad gap which insulates the two metal layers for carrier transport at the Fermi level. The barrier due to the band gap in the oxide is skewed due to an electric field across the oxide layer. Moreover, a bias voltage has been applied resulting in an offset of the Fermi levels of the two metals with respect to each other. The shading indicates the Fermi distribution of electrons at a finite temperature for the Ta layer and that the electronic system in the Au layer has been excited. The arrows indicate the energetically most probable situation for electron and hole transport, respectively.

The use of MIM devices to study chemical processes goes back to earlier work by Otto and coworkers in the context of electrochemistry.[17] Also the reverse process – hot electron driven surface chemistry utilising MIM devices – has received considerable interest.[18–21] In the applied world they receive interest as sensors.[22–24,26] For further reading we refer to the review by Bănică.[25]

3 Ultrahigh vacuum studies

Significant progress has been made in the last two decades in unravelling the fundamentals of gas-surface interaction.[6,27] Sophisticated experiments and rapid progress in theoretical modelling have contributed to this success.[28] Elaborate total energy calculations providing potential energy surfaces and high dimensionality quantum or classical calculations of the dynamics are today state-of-the-art. However, these schemes tacitly assume that the chemical process described evolves adiabatically in the

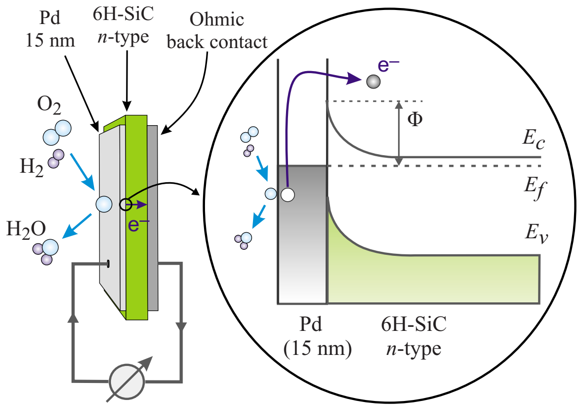

Fig. 3 Schematic drawing of the devices used by Karpov and coworkers and their respective bandstructure. The surface chemistry can induce hot electrons some of which are ballistically transported through the metal film and over the Schottky barrier in the Pd/n-SiC structure. Φ denotes the height of the Schottky barrier, E_C the position of the conduction band minimum, E_f the Fermi level, and E_V the top of the valence band. Reproduced from Ref. [15] with permission from 'Publisher AIP', [2015].

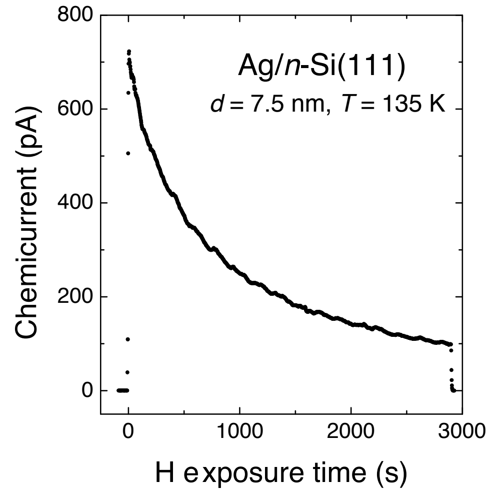

Fig. 4 "Chemicurrent" transient observed by Nienhaus and coworkers when exposing a Ag/n-Si(111) Schottky diode to a flux of H atoms. The device was held at 136 k and the thickness of the Ag layer was 7.5 nm. Adapted from Ref. [4] with permission from 'Publisher Elsevier', [2015].

electronic ground state. This is in particular the case whenever density functional theory (DFT) is relied upon. In order to cope with the many nuclear degrees of freedom involved in surface processes, schemes are advantageous which calculate the potential data points ad hoc along with the evolution of a trajectory, for which the term ab initio molecular dynamics (AIMD) has been coined.[29,30] There is, however, mounting evidence suggesting that non-adiabatic effects must not be neglected in many important situations.[5,31] Experiments, such as the dissociative adsorption of O_2 on Al(111)[32–35] and the interaction of highly vibrationally excited NO with Cu(111)[36] and Cs covered Au(111)[37] raise the question whether the non-adiabaticity in surface chemical reactions has not been underestimated in the past. The significance of non-adiabatic effects in dissociative adsorption or recombinative desorption is lively and controversially discussed[38,39] based on studies of interaction systems such as H_2/Cu(111),[40–43] N_2/Ru(001)[41,44,45] and N_2/W(110).[42] On the theoretical side, first steps have been undertaken to cope with this challenge.[46–51]

Naturally, there is a quest to have a direct measure of the degree of non-adiabaticity in gas-surface interactions. In seminal work, Nienhaus and coworkers reported the observation of a *chemicurrent* when a Ag/Si-Schottky diode was exposed to a flux of hydrogen atoms suggesting that a portion of the chemisorption energy is dissipated to electronic degrees of freedom of the substrate.[52] This experiment has stimulated novel theoretical studies.[53–58]

The experiment of Nienhaus and McFarland showed an initial electron flux of 4.5×10^{-4} e^- per adsorbing H atom (Fig. 4). The signal decreased exponentially with time which was attributed to the saturation of surface sites with H adatoms. The steady-state current was attributed to the fact that sites became available again due to Eley-Rideal type abstraction reactions.

Nienhaus and coworkers have build on their initial work on hydrogen adsorption[52,59] by using Metal/Si Schottky diodes to study the oxidation of alkali[60] and Mg films[61] as well as the homoepitaxy of Mg.[62]

In our laboratory we have used MIM structures to search for electronic excitations in the course of the interaction of H with and on metal surfaces.[8–10] Studies could be carried out over the temperature range from 130 to 350 K due to the negligible sensitivity to visible photons and the smaller thermal noise level of MIMs. Au was the material primarily used for the catalytic surface. The results were later on compared to those obtained with other metals, such as Cu, Ag and Pt.

Analysing the current transients and correlating them with the kinetics of the hydrogen recombination reaction, the following observations could be established: (*i*) The steady-state current follows the same rate law as the recombinations reaction. (*ii*) If the flux of hydrogen atoms is cycled, the observed transient is in agreement with 2nd order kinetics for the recombination reaction. (*iii*) A contribution from adsorption or Eley-rideal type abstraction events can only be of minor importance although it cannot completely be ruled out. (*iv*) With the build up of coverage a displacement current is observed, which is due to the shift of the Fermi level in a nanometer thick metal film when adsorption is accompanied by charge transfer at the surface. (*v*) The signal scales with the thickness of the top metal layer as it is expected from the free path length of electrons at an energy corresponding to the barrier height. Hence, the data suggests that the Langmuir-Hinshelwood type recombination events are the predominating source of electronic excitations which are observed as current.

The currents were found to scale as expected when the substrate metal was varied from which the oxide layer was prepared. Al exhibits such a high barrier (2-3 eV depending on preparation method)[12] that no current could be observed. Using Ti instead of Ta, a significantly larger current resulted as the barrier is smaller with 1.2-1.4 eV compared to the 1.7 eV for Ta.[63]

At this point we may summarise: In Ag/Schottky barrier experiments at $T_S = 130$ K a chemicurrent is observed which is interpreted to result from H atom adsorption. In experiments using MIM devices at elevated temperatures a current arising from the LH recombination reaction dominates. These two reports conflict on first glance, but may not necessarily do so. At $T_S = 130$ K the recombination reaction has a very small rate such that a current may escape observation in the Nienhaus experiments. Moreover, it may be speculated that a current from the recombination reaction contributes to the steady-state current reported. Experiments at elevated temperature have not been feasible with Schottky diodes due to the thermal noise. In the experiments using MIM devices, on the other hand, the electronic excitations arising from adsorption may not have been observable due to the higher barrier in these devices. This reasoning would suggest that H adsorption leads to excitation of smaller mean energy than those from the LH recombination reaction. This argument is corroborated by the fact that the current density observed with Schottky devices is about one order of magnitude larger than the one seen with MIM devices. Interestingly, Wodtke and coworkers have recently found evidence that the creation of electron-hole pairs mediates strong energy losses in the collision of hyperthermal H atoms with a Au surface.[64] Theoretical modelling suggests that the H atoms undergo sequential collisions transferring on average 0.4 eV each time,[65] which would be consistent with the interpretation of the MIM and Schottky device experiments.

Studying different metals as substrate for the chemistry we found: For the coinage metals – Ag and Cu – the findings are qualitatively equal to the ones discussed for Au, but quantitatively different. In contrast, no chemicurrent attributable to the recombination reaction could be observed for Pt.

The interaction of hydrogen with coinage and noble metal surfaces has been subject of innumerable studies.[66] The binding energy of H with the various faces of these metals ranges between 260 - 280 kJ/mol for Pt, 230 kJ/mol for Cu, and 190 - 210 kJ/mol for Ag and Au.[67] Whereas these differences seem only quantitative in nature, the transition state to recombinative desorption has a different character in the case of Pt group metals when compared to the coinage metals.[68] In the latter case the transition state lies energetically 50 to 100 kJ/mol above the asymptotic level corresponding to an unbound H_2 molecule, with the highest value expected for Au. In the case of Pt, there is no such pronounced maximum in the minimum energy path way of the molecule away from the surface.[69] This is inline with the finding that dissociative H_2 adsorption is not activated on Pt group metals, whereas on coinage metal it is strongly.

When using both kinds of devices – MIM sensors or Schottky contacts – marked isotope effects are observed. The signal for H exposure is by a factor of about 4 larger than for D exposure.[8,59] A strong isotope effect is generally seen as a litmus test for non-adiabaticity. The influence of non-adiabatic coupling scales with the velocity of the particle. Hence, comparing two isotopes at the same translational energy the amount of energy lost due to non-adiabatic effects scales with the square root of the mass ratio. This expectation is reproduced in first principles model calculations using time-dependent DFT.[70] As the barrier in the device cuts off low energy excitations, large isotope effects result. Knowing the cut-off energy and assuming a Boltzmann distribution, the parameter characterising this distribution can be derived, which is often expressed as a fictitious temperature. In these studies values between 2000 and 3000 K are found. If this value is for the moment interpreted as the mean energy of the excitations, then this amounts to some 10 kJ/mol, i.e. a tenth of a typical chemical binding energy. Interestingly, the reported isotope effect by Nienhaus and coworkers in their experiment is smaller than the one reported by us for experiments using MIMs which is inline with the suggestion that adsorption results in excitations of lower energy than the recombination reaction.

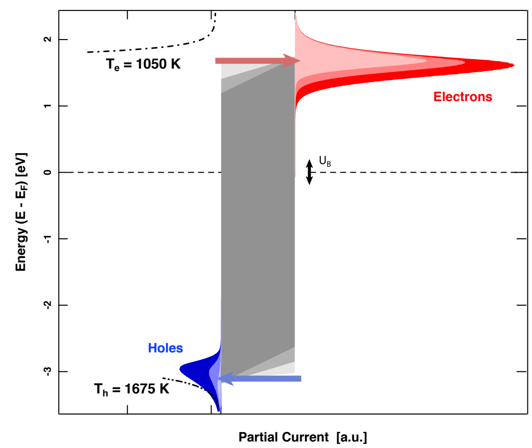

Fig. 5 Differential Spectroscopy of the energy distribution of the electron and hole flow in MIM device. By biasing the device the two Fermi levels are offset with respect to each other. As a consequence electron and hole flow are eased or hampered. Form the current variation the slop of the energy distribution in the vicinity of the cut-off energies can be derived; 1075 K and 1675 K for the electron and the holes, respectively.

MIM devices allow one to apply a bias voltage between the two metal layers. As a consequence the Fermi levels are shifted with respect to each other and the barrier imposed by the band gap in the oxide is distorted (Fig. 1). Depending on polarity, transport from the top layer to the back contact becomes easier for electrons or alternatively holes, while the other type of carriers encounters the opposite effect. Effectively, the median cut-off energies are shifted to lower values on the absolute energy scale or to higher ones. Alternating the applied allowed bias voltage allows to obtain the derivative of the current with respect to the cut-off energy, that is the spectrum in the vicinity of these energy values (Fig. 5). Experiments for H interacting with Au yielded that the distribution of electrons has a slope of 1050 K at an energy of 1.4 eV and the one for holes of 1675 K at the cutoff-energy of 2.4 eV. For D atom dosing smaller values, namely 900 and 1050 K, respectively, were found as expected. These values give a refined picture of the respective distributions when compared to the simple estimate derived from the isotope effects.

Theoretical work has focused on the non-adiabaticity of atomic hydrogen adsorption. The crossing of the atomic affinity level through the Fermi level of the metal is seen as the critical point along the trajectory as it gives rise to a spin orthogonalisation catastrophe when discussed within the Newns-Anderson picture.[54–57] The later arises as the H atom carries spin but the metal is spin umpolarized. Qualitative agreement has been achieved in model calculations. Less theoretical attention has been paid to the recombination process. But recent work has suggested that motion of hot H atoms on the surface may be connected with large electronic friction.[48] Such motion is the precursor to any recombination reaction and, hence, would scale with the rate of this reaction.

4 Higher pressure studies

Studies at pressures large enough to induce in thin film structures currents of macroscopically relevant magnitude have been pioneered by the Somorjai group.[71–73] For their initial studies they used structurally rather complicated Pt/TiO_2 and Pt/GaN devices for which they coined the term catalytic nanodiode. Exposing these devices to a near-stoichiometic flow of CO + O_2 at about 10^4 Pa and elevating the temperature to 400 to 550 °C, they observed for hours steady currents. In a subsequent study of the hydrogen oxidation reaction,[74] a yield of 1.1×10^{-4} electrons per reaction event was derived, by looking at the ratio of the current observed to the turnover frequency (Fig. 6). One question of concern was: what is the thermoelectric contribution to these currents. This question was addressed by running experiments in which the devices were exposed a flow of He. However, it is difficult to account this way for the heating due to the dissipated exothermicity of the chemical reactions.

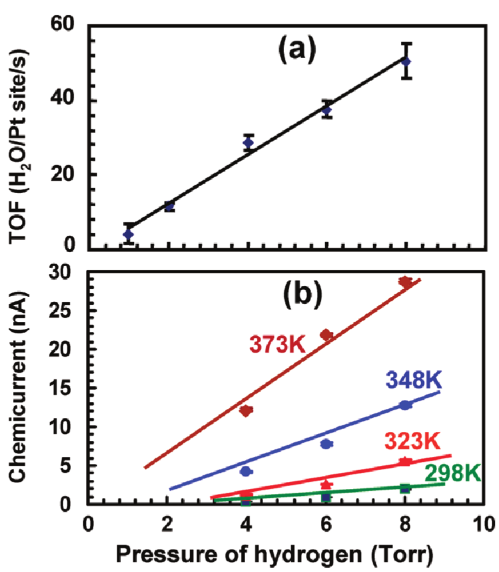

Fig. 6 Turnover frequency for different pressures of H_2 in 10^5 Pa of O_2 at 353 K. (b) A plot of the chemicurrent as a function of different H_2 pressures in 10^5 Pa of O_2. Reprinted with permission from[74]. Copyright (2009) American Chemical Society.

Karpov and Nedrygailov studied hydrogen oxidation to water on surfaces of Pd/n-SiC heterojunction nanostructures (Fig. 3).[15] These devices exhibit a Schottky barrier of 0.65 eV similar to the Si based ones, but the use of the wide band gap semiconductor SiC allows one to operate at elevated temperatures necessary to achieve appreciable reaction rates. Currents of up to 7.2 μA at T = 667 K were observed during admission of a stoichiometric oxygen-hydrogen mixture with a pressure of 25 Pa. Analysing their data, they concluded that the quantum yield may be as large as 0.2, whereby this property is defined as the number of electrons observed per water formation event. They suggested that the predominant part must be attributed to ballistic electrons as the current would be much larger than what is expected as thermionic current based on the Richardson equation.

In a subsequent paper the same authors employed Pd/GaP and Pt/GaP devices with results inline with their earlier conclusions.[3] In all these studies the prime argument was that the current observed scales linearly with the reaction rate.

Creighton and Coltrin[16] were able to shed some light on these experiments by building similar devices and modelling the heat flow in such a structure as used by Park and Somorjai. Arguing that the dominant source of a thermoelectric (Seebeck) current is the lateral temperature gradient between the two electric contacts, namely the Ohmic contact to the semiconductor substrate and the electric contact to the metal layer, a simplifying replacement circuit was constructed. Using experimentally determined temperatures for the two spots, a current is predicted which in magnitude and dependence on reaction rate agrees well with what is observed experimentally. The large current in these devices is facilitated by the large Seebeck coefficient of GaN.

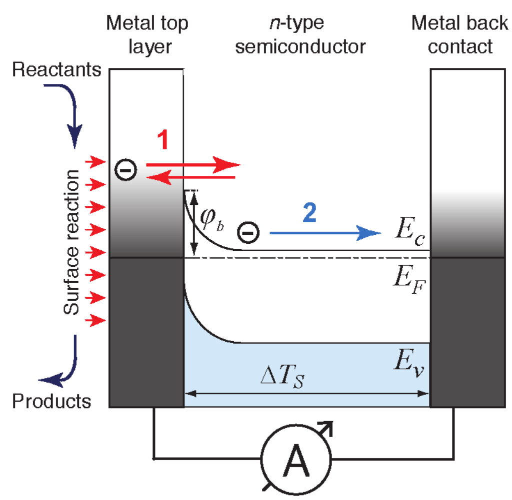

Fig. 7 Temperature gradients and resulting charge carrier transport in a metal-semiconductor nanostructure with φ_b the Schottky barrier height, E_F the Fermi level, δT_S the temperature drop across the semiconductor layer, and E_C and E_V the conduction band minimum and valence band top energy, respectively. A thermionic current (1) arises in case of a temperature drop across the metal-semiconductor interface. The thermoelectric current (2) is due to the Seebeck effect caused by the temperature gradient across the semiconductor layer between the interfaces to the top metal layer and the Ohmic metal back contact.

Three possible origins have to be considered for any chemicurrent: (*i*) the kind of current we discussed for the UHV studies, namely a *true* chemicurrent arising from electrons, respectively holes, excited in the context of a chemical reaction event and ballistically transported to the internal interface. (*ii*) a *thermionic* current arising from a difference in temperatures between the two metal layers which are separated by the barrier. (*iii*) a *thermoelectric* current arising from a temperature gradient across any one of the layers due to the finite thermal conductivity. If the two layers separated by the oxide barrier are of different temperature an imbalance in their respective (Fermi) distribution of carriers arises. In thermal equilibrium the electron flows from one layer to the other and vice versa cancel. In case of a temperature gradient, this is not anymore the case as the hotter layer will contribute a larger number of electrons ("1" in Fig.7). Hence, a macroscopic current arises as long as the two layers are shortcircuited. Quantitatively, this current can be accounted for by applying the Bethe equation

$$J_{1\to 2} = AT_1^2 \exp\left[-\frac{e\varphi_b}{k_B T_1}\right], \tag{1}$$

where A is the Richardson constant, φ_b the Schottky barrier height and δT_1 the temperature of the emitting layer. The major uncertainty is the Richardson constant one needs to know, what however is only truly the case for metals. The macroscopic current is then the difference between the microscopic ones in both directions.

Thermoelectric currents inside one medium arise due to temperature differences between two boundary surfaces of one medium. The driving force for these currents is the Seebeck voltage which is induced by a diffusion process of thermally activated charge carriers.[75] The dominating charge carriers (electrons in metals in and n type semiconductors, defect electrons in p-type semiconductors) flow from the hotter edge of the medium to the colder giving to rise a potential difference between the edges of the medium. Non-negligible temperature differences across a medium can be expected when one interface of the medium is heated by the catalysed reactions while the other side is ultimately connected to a heat sink. Such kind of devices were introduced decades ago.[76] When the surface of such a device supports a catalyzed reaction with a significant turn over frequency, a heat flow of several 10 mW/cm^2 is to be expected.[77] The resulting temperature gradient can lead to significant thermoelectric currents in particular across semiconductor layers. For silicon the Seebeck coefficient is in the range of 1000 μV/K,[76] for Ga based systems one finds 300 μV/K.[78] Even in the latter case the Seebeck coefficient is large enough to expect device currents of the size which have been attributed in some studies to chemiscurrents.[16]

As the top layer is only nanometers thick, no significant temperature drop will exist across it. The same argument holds for the insulating oxide layer in MIM devices. Thus, a thermoelectric current has only to be considered for the back electrode. The comparably low contribution of thermoelectric effects is to be expected for these MIM devices as the Seebeck coefficient is small for metals.[79] For noble metals the Seebeck coefficient does not exceed 10 μV/K, for the catalytically active platinum the coefficient even becomes zero at 200 K and changes sign.[80]

In any case, the exothermicity of the chemistry at the vacuum interface is a significant power source causing a temperature gradient across the device, the details of which depend on its design and its suspension in the apparatus. When the back electrode is made from a material with a large Seebeck coefficient such as most semiconductors, this will be the largest concern. For MIM devices the thermionic current is likely dominating as the Seeback coefficients of metals are small.

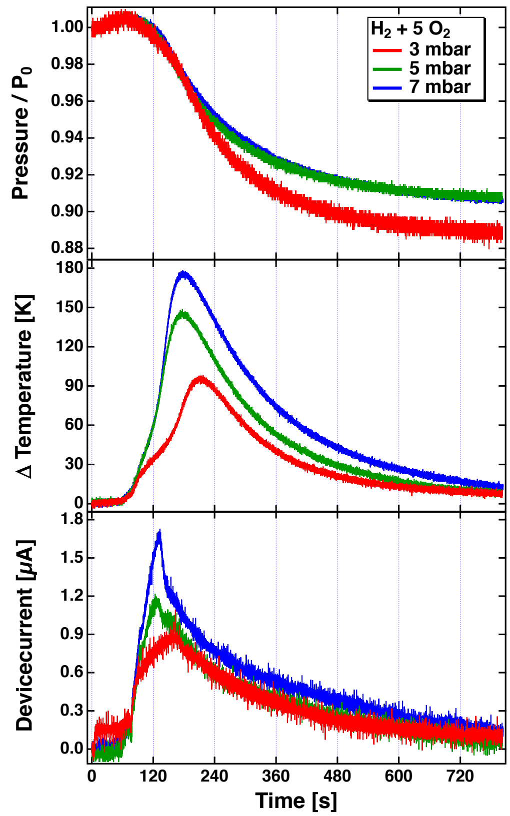

Fig. 8 Pressure, temperature increase and device current observed during the reaction of H_2 with O_2 in a bulb experiment using a Pt/Si device. The bulb (55 *l*) was filled with H_2 and O_2 in the ratio of 1:5 to total pressures of 3, 5 and 7 mbar. The reaction was initiated at about t= 80 s by irradiating the Pt surface with a light bulb which causes the temperature to rise from room temperature to the ignition one.[81]

The problem becomes immediately apparent when one inspects the results depicted in Fig. 8. These have been obtained in a bulb experiment using mixtures of H_2 and O_2 in the ratio 1:5 at different pressures.[81] The experiment used a Pt/SiOx/Si device. The reaction was started by radiatively heating the Pt film after the gas volume had been filled with the mixture. The top panel shows the evolution of the pressure over time as the reaction proceeds. The rate of the reaction is largest where the descent of the pressure is steepest. This agrees well with the temperature increase which is read using a tiny Pt1000 sensor attached to the Pt film. The device was hang from thin wires to reduce the heat conduction as far as possible, and thereby minimise temperature gradients in the device. The bottom panel depicts the temporal evolution of the current. A true chemicurrent one would expect to occur synchronous with the chemical rate. It is immediately obvious, that it evolves differently than the temperature measured and as the rate of the chemical reaction. The peak current is observed earlier in time. This experiment clearly suggests that the current cannot solely by attributed to electrons excited in the course of the surface chemical reactions. But it also does not appear be only a temperature effect.

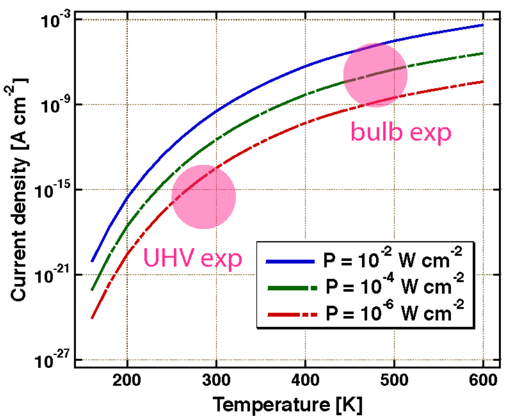

Fig. 9 Thermoelectric current density as calculated using a simple model for a Pt/Si device. It is assumed that the Si substrate is 0.5 mm thick. The temperature at the backside of the device is the variable. Three different amounts of power dissipated from a catalysed chemical reaction on the surface are considered, 10^{-2}, 10^{-4} and 10^{-6} W cm^{-2}. The coloured circles indicate the regimes in which typical UHV and bulb experiments are operated. Adapted from Ref. [77].

Nedrygailov et al. have addressed this problem in model studies.[77] Considering a Pt/n-Si device for which the thickness of the Si substrate is 0.525 mm, he calculated the thermionic and thermoelectric current. The chemistry proceeding at the vacuum interface is regarded as a power source. Typical turn-over-frequencies in bulb experiments correspond to 10^{-4} to 10^{-2} W cm^{-2}. For simplicity is assumed that the backside is uniformly held at a fixed temperature by the experimental layout allowing for a one-dimensional model. The first finding is that the thermoelectric current is by two orders of magnitude larger than the thermionic one. The size of the first markedly depends on the temperature at the back of the device (Fig. 9). Between 200 and 600 K a variation of the current over 12 orders of magnitude is calculated. For conditions typical of bulb experiments, the model predicts a current density of 10^{-9} to 10^{-5} A/cm^2. This result is remarkable as the temperature difference across the backelectrode ranges only between 10^{-6} to 10^{-3} K.

Admittedly, the thermoelectric effect is more pronounced in Si-devices than e.g. GaN or TiO_2 based ones. But it raises certainly concern, that the model suggests currents of a size as typically observed in the bulb experiments. On the other hand, it is reassuring that under UHV experimental conditions thermoelectric currents between 10^{-17} to 10^{-14} A/cm^2 are to be expected.

At present, the largest experimental stumbling block is an accurate *insitu* measurement of the temperature of the catalytic active nano film. With a volume of typically 0.1 mm3 its heat capacity is orders of magnitude smaller than the one of the smallest sensor, such as a Pt1000. Optical measurement are hampered by the fact that such thin metal films are optically partially transparent. Indirect ways to measure this temperature have been explored,[82,83] but they must not conflict with recording the *chemicurrent*.

5 Conclusions

Thin film metal heterostructures have allowed to shed new light on the dissipation of chemical energy into electric excitations on metal surfaces. The findings challenge the unreflected assumption that surface chemical process will in any case be adiabatic, i.e. follow the ground state potential energy surface. Encouraging strides have been made to account by theoretical work for these experimental findings. Regarding the work under high pressure conditions it has been found that it is harder than expected to separate direct electronic from subsequent thermal effects. The search for materials with larger conversion efficiencies is still on.

References

1 P. W. Anderson, *Phys. Rev. Lett.*, 1967, **18**, 1049.
2 X. Ji, A. Zuppero, J. M. Gidwani and G. A. Somorjai, *Nano Lett.*, 2005, **5**, 753.
3 E. G. Karpov and I. Nedrygailov, *Phys. Rev. B*, 2010, **81**, 205443.
4 H. Nienhaus, *Surf. Sci. Rep.*, 2002, **45**, 1 – 78.
5 E. Hasselbrink, *Curr. Opin. Solid State Mater. Sci.*, 2007, **10**, 192 – 204.
6 K. Golibrzuch, N. Bartels, D. J. Auerbach and A. M. Wodtke, *Annu. Rev. Phys. Chem.*, 2015, **66**, 399.
7 J. Y. Park, L. R. Baker and G. A. Somorjai, *Chem. Rev.*, 2015, **115**, 2781.
8 B. Mildner, E. Hasselbrink and D. Diesing, *Chem. Phys. Lett.*, 2006, **432**, 133.
9 B. Schindler, D. Diesing and E. Hasselbrink, *J. Phys. Chem. C*, 2013, **117**, 6337.
10 B. Schindler, D. Diesing and E. Hasselbrink, *J. Chem. Phys.*, 2011, **134**, 034705.
11 D. Diesing, A. W. Hassel and M. M. Lohrengel, *Thin Solid Films*, 1999, **342**, 282.
12 D. A. Kovács, J. Winter, S. Meyer, A. Wucher and D. Diesing, *Phys. Rev. B*, 2007, **76**, 235408.
13 K. Stella, D. A. Kovács, D. Diesing, W. Brezna and J. Smoliner, *J. Electrochem. Soc.*, 2011, **158**, P65.
14 P. Thissen, B. Schindler, D. Diesing and E. Hasselbrink, *New. J. Phys.*, 2010, **12**, 113014.
15 E. G. Karpov and I. I. Nedrygailov, *Appl. Phys. Lett.*, 2009, **94**, 214101.
16 J. R. Creighton and M. E. Coltrin, *J. Phys. Chem. C*, 2012, **116**, 1139.
17 D. Diesing, G. Kritzler, M. Stermann, D. Nolting and A. Otto, *J. Solid State Electrochemistry*, 2003, **7**, 389.
18 R. G. Sharpe, S. Dixon-Warren, P. Durston and R. Palmer, *Chem. Phys. Lett.*, 1995, **234**, 354.
19 J. W. Gadzuk, *Phys. Rev. Lett.*, 1996, **76**, 4234.
20 D. Diesing, H. Janssen and A. Otto, *Surf. Sci.*, 1995, **331/3**, 289.
21 T. Wadayama, A. Kojim and A. Hatta, *Appl. Phys. A*, 2004, **79**, 1891.
22 K. I. Lundstrom, M. S. Shivaraman and C. M. Svensson, *J.*

Appl. Phys., 1975, **46**, 3876–3881.

23 L.-G. Ekedahl, M. Eriksson and I. Lundstrom, *Acc. Chem. Res.*, 1998, **31**, 249.

24 H. Nienhaus, H. S. Bergh, B. Gergen, A. Majumdar, W. H. Weinberg and E. McFarland, *J. Vac. Sci. Technol. A*, 1999, **17**, 1683.

25 F.-G. Bănică, in *Chemical sensors based on semiconductor electronic devices*, John Wiley & Sons, Ltd, 2012, pp. 217–245.

26 D. Sarkar, H. Gossner, W. Hansch and K. Banerjee, *Applied Physics Letters*, 2013, **102**, 023110.

27 G. R. Darling and S. Holloway, *Rep. Prog. Phys.*, 1995, **58**, 1595.

28 *Handbook of Surface Science*, ed. E. Hasselbrink and B. I. Lundqvist, Elsevier, Amsterdam, 2008, vol. 3.

29 M. C. Payne, I. Stich, A. D. Vita, M. J. Gillan and L. J. Clarke, *Faraday Discuss. Chem. Soc.*, 1993, **96**, 151.

30 C. Díaz and G. J. Kroes, in this volume.

31 A. M. Wodtke, J. C. Tully and D. J. Auerbach, *Int. Rev. Phys. Chem.*, 2004, **23**, 513.

32 A. J. Komrowski, J. Z. Sexton, A. C. Kummel, M. Binetti, O. Weiße and E. Hasselbrink, *Phys. Rev. Lett.*, 2001, **87**, 246103.

33 M. Binetti and E. Hasselbrink, *J. Phys. Chem. B*, 2004, **108**, 14677.

34 J. Behler, K. Reuter and M. Scheffler, *Phys. Rev. B*, 2008, **77**, 115421.

35 F. Libisch, C. Huang, P. Liao, M. Pavone and E. A. Carter, *Phys. Rev. Lett.*, 2012, **109**, 198303.

36 Y. Huang, C. T. Rettner, D. J. Auerbach and A. M. Wodtke, *Science*, 2000, **290**, 111.

37 J. D. White, J. Chen, D. Matsiev, D. J. Auerbach and A. M. Wodtke, *Nature*, 2005, **433**, 503.

38 A. Hodgson, *Prog. Surf. Sci.*, 2000, **63**, 1.

39 P. Nieto, E. Pijper, G. Laurent, R. A. Olsen, E. J. Baerends, G. J. Kroes and D. Farias, *Science*, 2006, **312**, 86.

40 A. C. Luntz, M. Persson and G. O. Sitz, *J. Chem. Phys.*, 2006, **124**, 091101.

41 A. C. Luntz and M. Persson, *J. Chem. Phys.*, 2005, **123**, 074704.

42 J. I. Juaristi, M. Alducin, R. D. Muiño, H. F. Busnengo and A. Salin, *Phys. Rev. Lett.*, 2008, **100**, 116102.

43 A. S. Muzas, J. I. Juaristi, M. Alducin, R. D. Muiño, G. J. Kroes and C. Díaz, *J. Chem. Phys.*, 2012, **137**, 064707.

44 L. Diekhöner, L. Hornekær, H. Mortensen, E. Jensen, A. Baurichter, V. V. Petrunin and A. C. Luntz, *J. Chem. Phys.*, 2002, **117**, 5018.

45 C. Díaz, J. K. Vincent, G. P. Krishnamohan, R. A. Olsen, G. J. Kroes, K. Honkala and J. K. Nørskov, *J. Chem. Phys.*, 2006, **125**, 114706.

46 N. Shenvi, S. Roy and J. C. Tully, *J. Chem. Phys.*, 2009, **130**, 174107.

47 S. Monturet and P. Saalfrank, *Phys. Rev. B*, 2010, **82**, 075404.

48 M. Blanco-Rey, J. I. Juaristi, R. D. Muiño, H. F. Busnengo, G. J. Kroes and M. Alducin, *Phys. Rev. Lett.*, 2014, **112**, 103203.

49 K. Golibrzuch, P. R. Shirhatti, I. Rahinov, A. Kandratsenka, D. J. Auerbach, A. M. Wodtke and C. Bartels, *J. Chem. Phys.*, 2014, **140**, 044701.

50 M. Grotemeyer and E. Pehlke, *Phys. Rev. Lett.*, 2014, **112**, 043201.

51 A. Wodtke, in this issue.

52 H. Nienhaus, H. S. Bergh, B. Gergen, A. Majumdar, W. H. Weinberg and E. W. McFarland, *Phys. Rev. Lett.*, 1999, **82**, 446 – 449.

53 J. W. Gadzuk, *J. Phys. Chem. B*, 2002, **106**, 8265 – 8270.

54 J. R. Trail, M. C. Graham, D. M. Bird, M. Persson and S. Holloway, *Phys. Rev. Lett.*, 2002, **88**, 166802.

55 M. Lindenblatt and E. Pehlke, *Phys. Rev. Lett.*, 2006, **97**, 216101.

56 D. M. Bird, M. Mizielinski, M. Lindenblatt and E. Pehlke, *Surf. Sci.*, 2008, **602**, 1212–1216.

57 M. S. Mizielinski, D. M. Bird, M. Persson and S. Holloway, *Surf. Sci.*, 2008, **602**, 2617.

58 M. Timmer and P. Kratzer, *Phys. Rev. B*, 2009, **79**, 165407.

59 D. Krix, R. Nünthel and H. Nienhaus, *Phys. Rev. B*, 2007, **75**, 073410.

60 D. Krix and H. Nienhaus, *Appl. Surf. Sci.*, 2013, **270**, 231.

61 S. Glass and H. Nienhaus, *Phys. Rev. Lett.*, 2004, **93**, 168302.

62 U. Hagemann, M. Timmer, D. Krix, P. Kratzer and H. Nienhaus, *Phys. Rev. B*, 2010, **82**, 155420.

63 K. Stella, *PhD thesis*, Universität Duisburg-Essen, 2011.

64 O. Bünermann, H. Jiang, Y. Dorenkamp, A. Kandratsenka, S. M. Janke, D. J. Auerbach and A. M. Wodtke, *Science*, 2015, **350**, 1346–1349.

65 S. M. Janke, D. J. Auerbach, A. M. Wodtke and A. Kandratsenka, *Journal of Chemical Physics*, 2015, **143**, 124708.

66 K. Christmann, in *Adsorbate properties of hydrogen on solid surfaces*, Springer, Berlin, 2006, vol. III/42A.5, p. 111.

67 P. Ferrin, S. Kandoi, A. U. Nilekar and M. Mavrikakis, *Surf. Sci.*, 2012, **606**, 679 – 68.

68 B. Hammer and J. K. Nørskov, *Surf. Sci.*, 1995, **343**, 211.

69 E. Pijper, G. J. Kroes, R. A. Olsen and E. J. Baerends, *J. Chem. Phys.*, 2002, **117**, 5885.

70 M. Lindenblatt and E. Pehlke, *Surf. Sci.*, 2006, **600**, 5068 – 5073.

71 X. Z. Ji and G. A. Somorjai, *J. Phys. Chem. B*, 2005, **109**, 22530–22535.

72 X. Ji, A. Zuppero, J. M. Gidwani and G. A. Somorjai, *J. Am. Chem. Soc.*, 2005, **127**, 5792–5793.

73 J. Y. Park and G. A. Somorjai, *ChemPhysChem*, 2006, **7**, 1409 – 1413.

74 A. Hervier, J. R. Renzas, J. Y. Park and G. A. Somorjai, *Nano Lett.*, 2009, **9**, 3930 – 3933.

75 T. H. Geballe and G. W. Hull, *Phys. Rev.*, 1955, **98**, 940–947.

76 W. Fulkerson, J. P. Moore, R. K. Williams, R. S. Graves and D. L. McElroy, *Phys. Rev.*, 1968, **167**, 765–782.

77 I. I. Nedrygailov, E. G. Karpov, E. Hasselbrink and D. Diesing,

J. Vac. Sci. Technol. A, 2013, **31**, 021101.

78 E. N. Hurwitz, M. Asghar, A. Melton, B. Kucukgok, L. Su, M. Orocz, M. Jamil, N. Lu and I. T. Ferguson, *J. Electron. Mater.*, 2010, **40**, 513–517.

79 B. Schindler, D. Diesing and E. Hasselbrink, *Z. Phys. Chem.*, 2013, **227**, 1381.

80 N. Cusack and P. Kendall, *Proc. Phys. Soc.*, 1958, **72**, 898.

81 I. I. Nedrygailov, D. Diesing and E. Hasselbrink, unpublished.

82 I. I. Nedrygailov, E. Hasselbrink, D. Diesing, S. K. Dasari, M. A. Hashemian and E. G. Karpov, *J. Vac. Sci. Technol. A*, 2012, **30**, 030601.

83 J. P. Meyburg, I. I. Nedrygailov, E. Hasselbrink and D. Diesing, *Rev. Sci. Instrum.*, 2014, **85**, 104102.

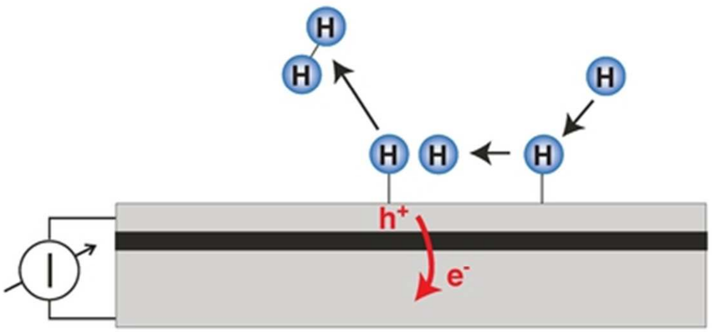

49x17mm (300 x 300 DPI)